JOURNAL OF AGRICULTURAL AND FOOD CHEMISTRY

High-Resolution NMR and Diffusion-Ordered Spectroscopy of Port Wine

MATHIAS NILSSON,† IOLA F. DUARTE,† CLÁUDIA ALMEIDA,† IVONNE DELGADILLO,† BRIAN J. GOODFELLOW,† ANA M. GIL,*,† AND GARETH A. MORRIS‡

Departamento de Química, Universidade de Aveiro, P-3810-193 Aveiro, Portugal, and Department of Chemistry, University of Manchester, Oxford Road, Manchester M13 9PL, U.K.

The use of high-resolution NMR and high-resolution diffusion-ordered spectroscopy (DOSY) for the characterization of selected Port wine samples of different ages with the aim of identifying changes in composition is described. Conventional 1D and 2D NMR methods enabled the identification of about 35 compounds, including minor components such as some medium-chain alcohols, amino acids, and organic acids. High-resolution (HR) DOSY extended sample characterization, increasing the number of compounds identified and NMR assignments made, by providing information on the relative molecular sizes of the metabolites present. Port wines of different ages were found to differ mainly in their content of (a) organic acids and some amino acids, (b) an unidentified possible disaccharide, and (c) large aromatic species. The relative amount of these last high M_w aromatics is seen to decrease significantly in the oldest wine, as expected from the known formation and precipitation of anthocyanin-based polymers during red wine aging.

KEYWORDS: NMR; DOSY; spectroscopy; Port wine; aging; aromatics

INTRODUCTION

Port wine is a well-known Portuguese product with worldwide commercial importance, its composition and properties being importantly related to the wine origin and age. In addition to the main constituents, water, ethanol, and monosaccharides, a large number of minor metabolites have been identified. Minor compounds such as alcohols, amino acids, and phenolic compounds are known to be of crucial importance for the characteristics of the wine and to change in concentration depending on age (*1*). In routine analysis of Port wine, many different methods such as gas chromatography, UV/vis spectroscopy, and chemical methods are normally used. High-resolution proton nuclear magnetic resonance (^{1}H NMR) spectroscopy has already proved of great value in the direct study of liquid foods such as fruit juices, beer, and wine (*2*−*13*). Its strength is that it provides qualitative and quantitative information in a rapid single experiment with minor sample preparation and in a noninvasive way. NMR of wine has been found useful for quality control purposes, for example, for the verification of wine origin, age, and adulteration effects, mainly in the form of site-specific natural isotopic fractionation (SNIF)-NMR, often in tandem with isotope-ration mass spectrometry (IRMS) (*10*−*12*); a review has been recently published on the subject (*13*). High-resolution NMR has the interesting potential of providing information on a wide variety of compounds, thus characterizing more thoroughly the chemical composition of the wine (*7*, *8*). However, the identification of compounds in such complex mixtures by ^{1}H NMR alone is frequently hindered by severe signal overlap and by the weak intensity of some resonances. The aromatic regions of the spectra are particularly difficult to assign due to these problems. The use of two-dimensional (2D) NMR adds information on correlation between resonances and, by dispersing the signals in an extra dimension, decreases the problem of overlap, greatly facilitating the assignment procedure. Even so, weak signal intensity, signal overlap, or the lack of coupling information between different segments of a molecule often leads to ambiguous or incomplete assignments.

In this work, the NMR technique of high-resolution diffusion-ordered spectroscopy (DOSY) has been applied for the first time to the complex mixture of compounds that constitute Port wine to achieve improved interpretation of the composition changes between wines of different ages. DOSY is used to separate resonances according to the hydrodynamic radii of the corresponding compounds and may thus supply valuable information on the sizes of the molecules present. The principle of DOSY is to separate the NMR signals on the basis of their diffusion coefficients (*14*−*16*). A series of pulsed field gradient stimulated echo NMR spectra is recorded with increasing gradient pulse strength, resulting in signals decaying at rates determined by their diffusion properties. The signal decays are fitted to the appropriate theoretical expression to extract estimated diffusion

* To whom correspondence should be addressed: tel +351 234 370707; fax +351 234 370084; e-mail agil@dq.ua.pt.
† Universidade de Aveiro.
‡ University of Manchester.

10.1021/jf049797u CCC: $27.50
Published on Web 05/21/2004

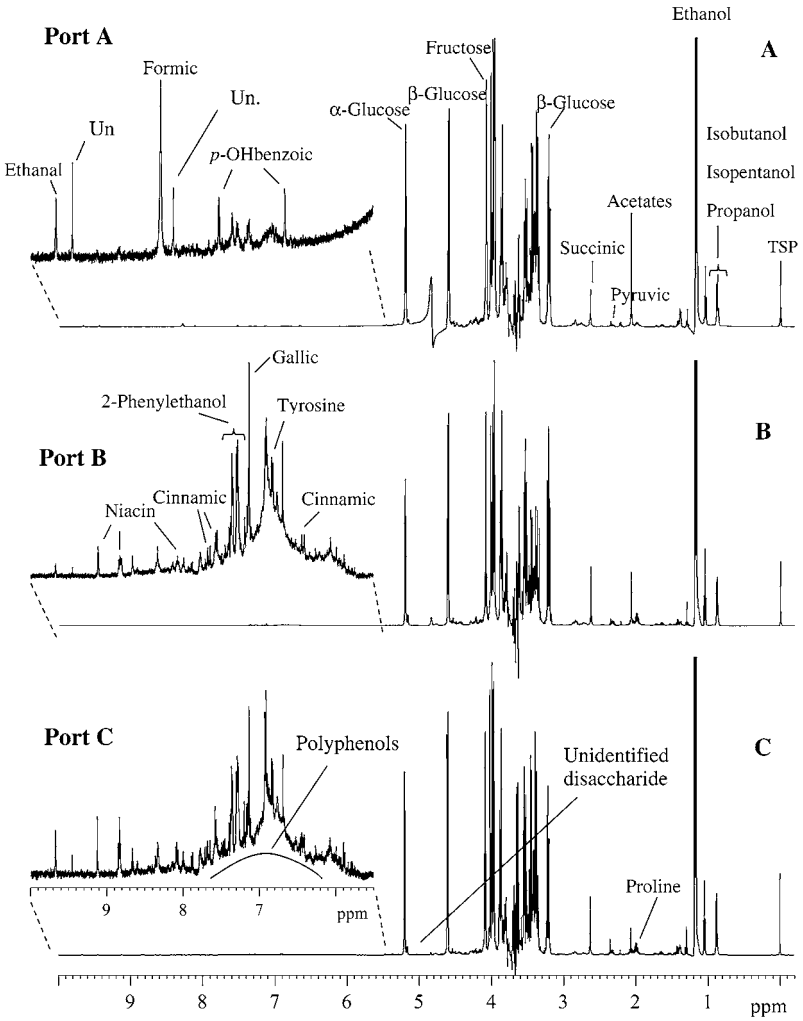

Figure 1. ^{1}H NMR spectra of (**A**) Port A (20 years old), (**B**) Port B (3 years old), and (**C**) Port C (1 year old), recorded with 128 transients. Some of the assigned resonances are indicated; signals marked "Un" remain unassigned.

coefficients. The DOSY spectrum is constructed with the original line shape for each signal in the spectral dimension and, in the diffusion dimension, a Gaussian line shape centered on the apparent diffusion coefficient and with a width determined by the standard error estimated in the fitting process. In high-resolution DOSY (*17*), the decays are fitted to single exponentials with two parameter fits. This can achieve resolution better than 1% in molecular size (hydrodynamic radius), but only for well-resolved signals; overlapped resonances give an apparent diffusion coefficient intermediate between those of the individual species concerned. DOSY spectra of liquid food samples have recently been reported for tomato juice (*18*), apple juice, grape juice, and beer (*19*), where it has been shown to assist in assignments and characterization of the samples.

MATERIALS AND METHODS

Samples. Port wines of three different ages were supplied by the Port Wine Institute, Porto, Portugal, and are hereafter identified as follows: Port A, 20 years old (pH 3.43); Port B, 3 years old (pH 3.70); Port C, 1 year old (pH 3.66). Although an attempt was made to choose similar wines as far as possible, differences in grape variety, characteristics of specific harvest year, and making and storage processes are naturally present. For each wine, the contents of one bottle were investigated; sample pretreatment consisted of the addition of D_2O and chemical shift reference sodium 3-(trimethylsilyl)-propionate-2,2,3,3-d_4 (TSP), resulting in a final concentration of 10% (v/v) D_2O and 0.0465% (w/v) TSP.

NMR and DOSY Experiments. High-resolution NMR spectra were recorded either on a Bruker Avance DRX-500 or on a Varian Unity 500 spectrometer, both operating at 500 MHz for ^{1}H. On the Bruker spectrometer, 1D ^{1}H NMR spectra were acquired using the NOESYPR1DSP pulse sequence (Bruker library) and processed with a line-broadening factor of 0.3 Hz. Suppression of the water and ethanol signals was achieved by applying a modulated shaped pulse during the relaxation delay (4.0 s) and the mixing time (100 ms). A total of 128 transients were collected into 8192 complex data points with a spectral width of 6009.62 Hz and an acquisition time of 1.36 s. On the Varian spectrometer, triple presaturation was achieved by gating both the transmitter and the decoupler on continuously at low level throughout the relaxation period of 2.0−4.0 s, the transmitter frequency being placed at the water resonance and the decoupler frequency being alternated every 48.7 ms between the ethanol CH_3 resonance at 1.17 ppm and the CH_2 resonance at 3.64 ppm. All experiments were carried out at 30 °C and nonspinning. Total correlation spectroscopy (TOCSY) spectra were acquired on the Bruker spectrometer in phase-sensitive mode using time proportional phase incrementation (TPPI) with an MLEV17 pulse sequence used for the spin-lock (*20*). A total of 1024 complex data points with 24−36 transients per increment and 256−512 increments were acquired with a spectral width of 6009.62 Hz in both dimensions, a mixing time of 100 ms, and a relaxation delay of 1 s. Heteronuclear single quantum coherence (HSQC) spectra were acquired with inverse detection, ^{13}C decoupling during acquisition, 1024 complex data points, 64−256 scans, 128−152 increments, and spectral widths of 6009.63 and 27 669.19 Hz in the ^{1}H and ^{13}C dimensions, respectively. Correlation spectroscopy (COSY) spectra were acquired on the Varian spectrometer using a gradient-selected coherence transfer

pathway (gCOSY) with two transients of 2048 complex data points, 1024 increments, a spectral width of 5499.79 Hz in both dimensions, and a relaxation delay of 2 s. 2D-*J* spectra were recorded using 48 transients of 4096 complex points, 64 increments, a relaxation delay of 3 s, and spectral widths of 5499.79 and 50 Hz in the ^{1}H (F_2) and *J* (F_1) dimensions, respectively.

2D ^{1}H DOSY spectra were acquired on the Varian spectrometer using the one-shot pulse sequence (*21*) with 19 gradient levels ranging from 6.4 to 25 G/cm and 128 transients of 16 384 complex points at each gradient level. The diffusion delay was 0.3 s, and the length of the square diffusion encoding gradient pulses was 2 ms; gradient stabilization time was 2 ms, and relaxation delay was 3.3 s. All calculations of DOSY spectra were done using a two-parameter monoexponential fit (HRDOSY) after cubic spline baseline correction. 2D DOSY data were corrected for the effects of imperfect field homogeneity by reference deconvolution (*22*, *23*). Each set of individual free induction decays was corrected with a generic target line shape (typically defined in the time domain by a rising exponential with a time constant of $^1/_\pi$ s and a decaying Gaussian with a time constant of 1 s) and stored. These data were then processed as normal with the time-domain weighting function adjusted to achieve a suitable compromise between resolution, line shape, and signal-to-noise ratio.

RESULTS AND DISCUSSION

The complexity of Port wine composition is clearly illustrated by the ^{1}H NMR spectra of the three wines of different ages shown in **Figure 1**. In all samples, the major signals arise in the 3.0−5.5 ppm region and originate from the monosaccharides glucose and fructose. Interestingly, as will be shown and discussed later, a number of additional anomeric peaks may be observed between 5.0 and 5.5 ppm, the assignment of which is hindered by signal overlap with the stronger carbohydrate resonances. Although some spectroscopic information is lost at 4.8 ppm (water) and at 1.17 and 3.64 ppm (ethanol) due to the effects of triple suppression of the water and the ethanol methyl and methylene signals, a great wealth of peaks may be observed in expansions of both aliphatic and aromatic regions. Based on the TOCSY, COSY, HSQC, and 2D-*J* spectra of all samples (not shown), the assignments indicated in **Figure 1** have been obtained; a complete list is given in **Table 1**.

The main components identified in the aliphatic region (0.5−3.0 ppm) of the NMR spectra of Port wine are acetic acid/acetates, succinic acid, pyruvic acid, lactic acid, and medium-chain alcohols (1-propanol, 2-methyl-1-propanol, 2-methyl-1-butanol, and 3-methyl-1-butanol), along with minor quantities of a few amino acids (**Table 1**). The main differences in the aliphatic regions of the three Port wines indicate for the oldest Port (Port A) slightly decreased concentrations of succinic acid (2.62 ppm), pyruvic acid (2.35 ppm), γ-butyric acid (GABA) (1.94 ppm), and proline (1.99, 2.06 ppm). It should be noted here that, in addition to the different wine ages, variables such as grape variety and differences in making process may contribute to some extent to changes observed in organic acid and amino acid composition. Port A also shows higher concentrations of lactic acid (1.38 ppm) and acetates (2.1 ppm) compared to the remaining wines. The composite acetate peak contains contributions from both acetic acid and acetate esters; this ambiguity is not resolved by the use of 2D NMR. The major contributor is acetic acid, which increases 3-fold from the youngest wine (Port C, 170 mg/dm^3) through Port B (220 mg/dm^3) to the oldest wine (Port A, 570 mg/dm^3), as determined by chemical analysis. Ethyl acetate should also contribute significantly to the acetate peak; again chemical analysis showed a 3-fold increase from Port C (36 mg/dm^3) to Port A (106 mg/dm^3). However, a contribution from additional acetates is likely to be present in the oldest wine (Port A) since the 2.1 ppm peak increases almost 5-fold between Port C and Port A. Finally, all three wines seem to contain similar concentrations of medium-chain alcohols, as reflected by the group of peaks at 0.9 ppm.

The main components identified in the sugar region (3.0−5.5 ppm) are glucose and fructose; the few weak additional anomeric peaks originating from minor carbohydrates are difficult to assign due to the strong signal overlap in 1D and 2D NMR spectra. **Table 1** shows that other compounds such

Table 1. ^{1}H and ^{13}C Chemical Shifts, Proton Multiplicity, and J_{HH} for Assigned Compounds in Port Wine[a]

compound	δ ^{1}H in ppm (multiplicity, *J* in Hz, assignment)/ δ ^{13}C in ppm
acetic acid/acetates	**2.06** (s, βCH_3)/23.42
alanine	**1.47** (d, 7.2, βCH_3)/17.17; **3.80** (αCH)/54.79
γ-aminobutyric acid (GABA)	**1.94** (βCH_2); **2.48** (αCH_2); **3.03** (γCH_2)
arginine	**1.68** (m, γCH_2); **1.90** (m, βCH_2); **3.22** (t, δCH_2)
caffeic/	**6.42** (d, 16.0, αCH); **6.91** (d, C5H);
trans-caftaric acid	**7.12** (d, C6H); **7.67** (d, 16.0, βCH)
citric acid	**2.75** (d, 16.4, α,γCH)/46.54;
	2.95 (d, 16.4, α',γ'CH)
p-coumaric/CCCC	**6.42** (d, 16.0, αCH); **6.91** (d, C3H/C5H);
trans-coutaric acid	**7.56** (d, C2H/C6H); **7.67** (d,16.0, βCH)
disaccharide	**5.16** (d, 3.9, C1H)/97.02
ethanal	**2.23** (d, 3.0, CH_3); **9.67** (q, CH)
ethanol	**1.17** (t, 7.2, CH_3)/19.56; **3.64** (q, 7.2, CH_2)/60.19
ethyl acetate[b]	**1.26** (t, 0.2, CH_3); **4.12** (q, 7.2, CH_2)
formic acid	**8.32**(s, *H*COOH)/169.8
α-fructose	**4.09** (C3H)/84.68
β-fructose	**4.09** (C3H, C4H)/77.56
gallic acid	**7.12** (s, C2H, C6H, ring)/112.37
α-glucose	**5.20** (d, 3.7, C1H)/95.15
β-glucose	**4.61** (d, 8.0, C1H)/99.10; **3.25** (dd, C2H)
p-hydroxybenzoic acid[b]	**6.67** (d, 3.3, C3H, C5H, ring)/113.7;
	7.54 (d, 3.3, C2H, C6H, ring)/129.9
isobutanol	**0.87** (d, 6.7, CH_3); **1.73** (m, CH);
(2-methyl-1-propanol)	**3.36** (d, CH_2OH)
isopentanol	**0.88** (d, 6.7, CH_3); **1.43** (q, CH);
(3-methyl-1-butanol)	**1.64** (CH_2); **3.61** (t, 6.7, CH_2OH)
lactic acid	**1.38** (d, 7.0, βCH_3)/22.41; **4.31** (q, αCH)
leucine	**0.95** (t, δ,δ' CH_3); **1.72** (βCH_2, γCH)
malic acid	**2.71** (dd, 6.0; 12.8, βCH)/39.48;
	2.82 (dd, β'CH); **4.45** (αCH)/69.81
methanol	**3.35** (s, CH_3)/46.15
2-methyl-1-butanol[b]	**0.87** (d, CH_3); **0.88** (t, CH_3);
	1.10 (m, 1/2CH_2); **1.38** (m, 1/2CH_2);
	1.53 (m, CH); **3.38** (dd, CH_2OH);
	3.47 (dd, CH_2OH)
niacin	**8.0** (dd, C5H); **8.82** (dd, C4H, C6H); **9.11** (C2H)
2-phenylethanol	**2.76** (CH_2); **3.74** (CH_2OH);
	7.28 (m, ring); **7.34** (m, ring)
proline	**1.99** (m, γCH_2)/26.40; **2.06** (β'CH)/31.57;
	2.33 (m, βCH)/31.57; **3.32** (δ'CH)/49.07;
	3.42 (δCH)/49.07; **4.11** (αCH)/63.76
1-propanol	**0.88** (t, 7.5, CH_3); **1.53** (m, CH_2);
	3.55 (t, 6.8, CH_2OH)
pyruvic acid[b]	**2.35** (s, βCH_3)
succinic acid	**2.62** (s, α, βCH_2)/31.74
tartaric acid[b]	**4.41** (s, αCH)
threonine[b]	**1.42** (γCH_3); **4.42** (βCH)
tyrosine/tyrosol	**6.83** (d, C3H, C5H, ring)/118.13;
	7.15 (d, C2H, C6H, ring)/133.30;
	6.87 (d, C3H, C5H, ring)/118.46;
	7.17 (d, C2H, C6H, ring)/133.80
uridine	**4.17** (C4′H); **4.29** (C3′H); **5.87** (C5H ring, C1′H);
	7.88 (C6H ring)

[a] s = singlet; d = doublet; t = triplet; q = quartet; dd = doublet of doublets; m = multiplet. [b] Tentative identification.

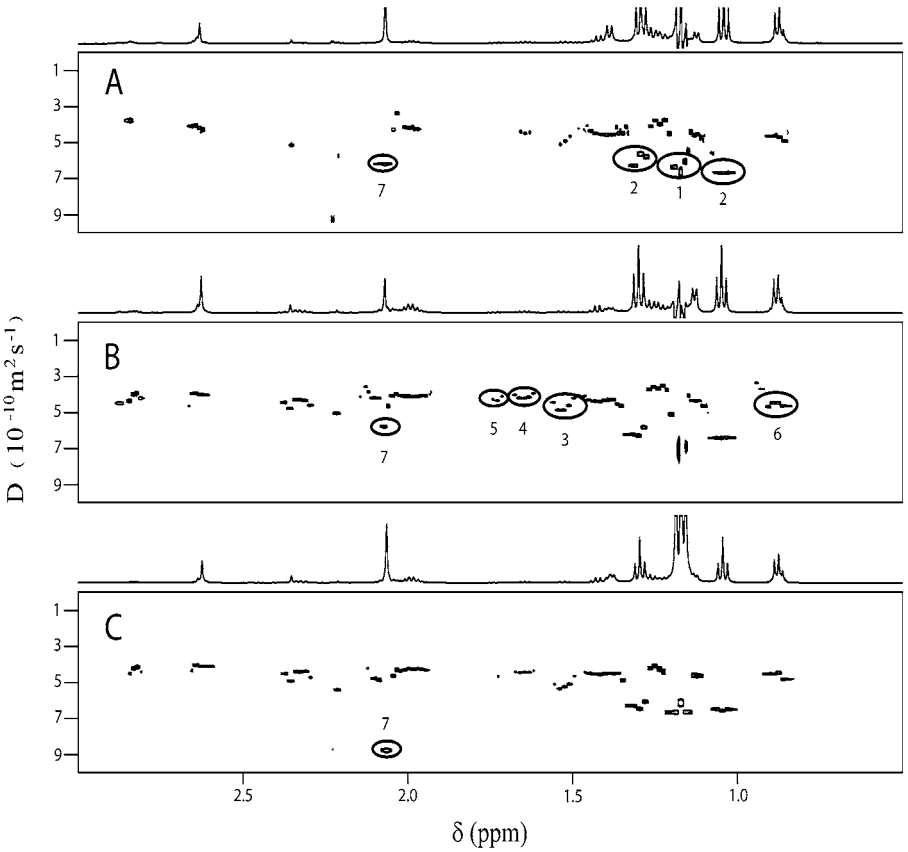

Figure 2. Aliphatic regions (0.5–3.0 ppm) of high-resolution DOSY spectra of (**A**) Port A (20 years old), (**B**) Port B (3 years old), and (**C**) Port C (1 year old). A proton spectrum measured with the one-shot DOSY pulse sequence with minimum pulsed field gradient amplitude is shown on top of each DOSY spectrum as a reference. The signals highlighted correspond to (1) ethanol, (2) ^{13}C satellites of ethanol, (3) 1-propanol and 2-methyl-1-butanol, (4) 3-methyl-1-butanol, (5) 2-methyl-1-propanol, (6) a mixture of signals 3–5, and (7) acetate(s).

as amino acids and alcohols also resonate in this region. The fructose/glucose ratio, as indicated by the area ratio of the β-glucose and fructose signals at 3.2 and 4.09 ppm, respectively (these signals were chosen to avoid any intensity disturbances caused by the solvent suppression), seems slightly lower for Port B but is similar for Ports A and C; therefore, no clear relation with age is found. In addition, an anomeric peak at 5.16 ppm is seen to decrease slightly from Port C to Port A, but its assignment is, at this point, unknown.

The aromatic region (5.5−10 ppm) shows clear changes (**Figure 1**) from Ports B and C to the oldest Port A, one of which is the decreased number of peaks resolved for Port A. A variety of aromatic species such as organic and amino acids (including gallic acid, cinnamic acid, tyrosine, niacin, caffeic/*trans*-caftaric acid, *p*-coumaric/*trans*-coutaric acid, and uridine) are present in Ports B and C, while the spectra of Port A show no significant evidence of these components. On the other hand, Port A is seen to be richer in ethanal, consistent with previous results (*1*) that showed an increase of ethanal with age due to ethanol oxidation, and in compounds such as formic acid and *p*-hydroxy benzoic acid, also showing higher intensity for the unidentified singlets at 8.12 and 9.45 ppm. In addition, the broad underlying components clearly observed in the younger Ports B and C are absent in Port A, suggesting precipitation or breakdown of large aromatic molecules over time. These findings are in agreement with the well-known formation and precipitation of polymeric pigments in red wines during aging (*24*, *25*). As wine ages, anthocyanins, responsible for the red color in young red wines, condense with other flavonoid compounds to give rise to polymeric pigments (*24*). The process is known to involve ethanal; most of the polymers precipitate and are therefore absent in older wines (*25*).

Although conventional 1D and 2D NMR allowed the identification of the compounds shown in **Table 1**, many signals remain unassigned in all regions of the spectra due to signal overlap, weak signal intensity, or both, as in the case of the aromatic region. High-resolution DOSY spectra were therefore measured in an attempt to augment the assignments achieved with 1D and 2D NMR. The DOSY spectra of the three wines have been split into the three spectral regions discussed above and are shown in **Figures 2**−**5**. Some caution is necessary in the interpretation and comparison of these spectra and of DOSY spectra in general. As noted above, where signals overlap a single apparent diffusion coefficient with a compromise value is seen. The apparent diffusion coefficients observed are strongly dependent on sample temperature and viscosity and can be misleadingly high if sample convection is present. In this study, sample temperature was regulated at 30 °C and samples were not found to convect. Any viscosity differences among the three wines were too small to detect, as shown by the very similar diffusion coefficients seen for TSP (3.65×10^{-10}, 3.56×10^{-10}, and 3.61×10^{-10} m^2/s for Ports A, B, and C, respectively, with an estimated standard error of 0.1×10^{-10} m^2/s).

Figure 2 shows the aliphatic regions of the DOSY spectra of the three Port wines. This region contains many signals from medium-chain alcohols, in addition to strong ethanol ^{13}C satellite signals and the residual ethanol methyl signal at 1.15 ppm (marked as signals 1 and 2, respectively, in **Figure 2A**). It is informative to look at the carbon satellites of ethanol since, in the absence of interfering effects, they should all show the same

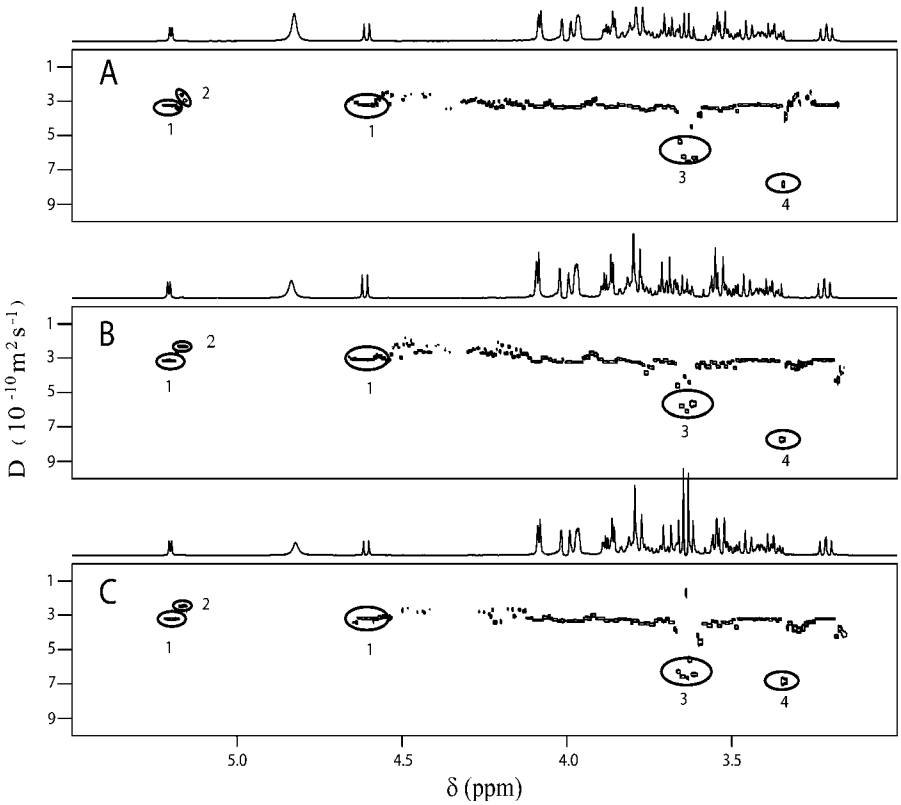

Figure 3. DOSY spectra of the 3.0–5.5 ppm region for (**A**) Port A (20 years old), (**B**) Port B (3 years old), and (**C**) Port C (1 year old). Some signals mentioned in the text are highlighted: (1) glucose, (2) unidentified possible disaccharide, (3) ethanol, and (4) methanol.

apparent diffusion coefficient. For the three wines studied, there is a reasonably good agreement in diffusion coefficients of the satellites, but the signals in the downfield multiplet show smaller apparent diffusion coefficients due to overlap with signals from more slowly diffusing species. The largest perturbation is that seen for Port A, probably due to overlap of the 1.3 ppm satellite with the peak of ethyl acetate at that chemical shift. The weak multiplets at 1.55, 1.65, and 1.75 ppm (signals 3−5) originate, respectively, from 1-propanol and 2-methyl-1-butanol, 3-methyl-1-butanol, and 2-methyl-1-propanol, which are present in all three wines although more clearly seen for Port B than for the other samples because of the choices of contour levels dictated by the dynamic ranges of the spectra. These signals are well resolved by diffusion coefficient, although the presence of small baseline errors means that the weak outer signals of the multiplets give slightly smaller apparent diffusion coefficients, an effect most clearly seen in **Figure 2B**. The signals in the multiplet cluster at 0.9 ppm (signal 6) also originate from these medium chain alcohols but are more poorly resolved in the spectral dimension and hence cannot be separated by their diffusion coefficients in this 2D DOSY experiment. Peak 7 shows a clearly larger apparent diffusion coefficient for Port C (9×10^{-10} m^2/s compared to 5×10^{-10} m^2/s), together with an apparently higher peak intensity compared to the spectrum shown for the same wine sample in **Figure 1C**. This is attributable to the contamination of the Port C sample prepared for the DOSY experiments by acetic acid from tube washes and offers an unintended illustration of the possibility of using DOSY to detect contamination even when the species concerned does not give a resolvable signal in the spectral dimension. Many additional DOSY peaks with diffusion coefficients similar to those of the alcohols identified are observed in all three samples for chemical shifts higher than 1.8 ppm; this confirms the assignment of signals in this region to medium-sized compounds compared with alanine at 1.47 ppm, lactic acid at 1.33 ppm, and pyruvic acid at 2.35 ppm and not to larger derivatives. As the above discussion indicates, the different ages of the Port wines do not significantly affect the aliphatic regions of their DOSY spectra.

The carbohydrate regions of the DOSY spectra, shown in **Figure 3**, similarly present no obviously significant differences among samples. Most signals between 3.3 and 4.2 ppm arise from ring protons of monosaccharides (mainly glucose and fructose), as shown by the agreement between their apparent diffusion coefficients and those of the anomeric signals at 4.6 and 5.2 ppm (glucose, signals marked 1) and at 4.1 ppm (fructose). The uniformity seen in the 3.3−4.2 ppm region is only broken by signals originating from the more rapidly diffusing ethanol at 3.65 ppm (signal 3) and nearby signals affected by overlap and methanol at 3.35 ppm (signal 4). A closer look at the anomeric region of the DOSY spectrum of Port B (expansion shown in **Figure 4**) shows the strong α-glucose anomeric signal at 5.20 ppm (signal 1) and its ^{13}C-satellites at 5.37 and 5.06 ppm (signals 2); the latter show good agreement, given the uncertainties caused by baseline correction and signal overlap, with the diffusion coefficient of the mother peak. In addition to the signal of the glucose anomeric proton, many other DOSY signals are seen that correspond to much weaker peaks in the 1D proton spectrum. There is an unidentified signal consistent with a monosaccharide anomeric proton at 5.47 ppm and a range of peaks from larger species. The strong signal at 5.17 ppm (signal 4 in **Figure 4**) is provisionally assigned to an unidentified disaccharide on the basis of its diffusion coefficient (2.1×10^{-10} m^2/s). Because the remaining signals are so much weaker, their apparent diffusion coefficients are much more vulnerable to systematic errors caused by imperfect baseline correction, and hence, it is not clear whether signals 5−8 correspond to disaccharides or larger species. Signal

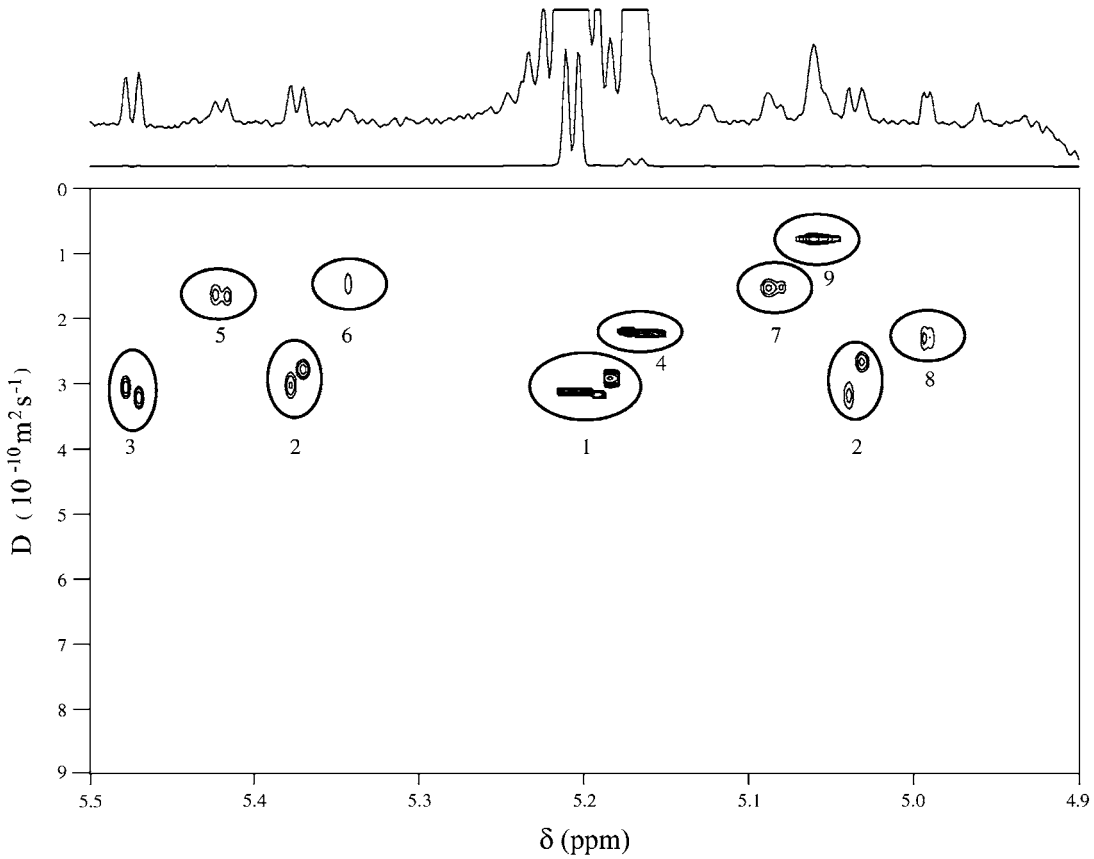

Figure 4. DOSY spectra of the anomeric proton region 4.9–5.5 ppm from Port wine B. Spectra were treated with digital filtration to reduce the residual water signal, Lorentz–Gauss resolution enhancement, and cubic spline baseline correction. Signals mentioned in the text are (1), glucose, (2) ^{13}C satellites of glucose, (3) unidentified monosaccharide, (4) unidentified disaccharide, (5–8) unidentified disaccharide or larger species, and (9) unidentified larger species.

9 at 5.07 ppm clearly originates in a species larger than a disaccharide; its apparent diffusion coefficient is consistent with a sugar−polyphenol conjugate, being the same as that of the most slowly diffusing aromatic signals around 7.0 ppm. However, the envelope of the soluble polyphenol signal is significantly weaker than signal 9, suggesting that the latter may have some other origin. Regarding compositional differences among the three Ports, no clear differences can be seen by DOSY in terms of their sugar composition. However, DOSY does allow the peak at 5.17 ppm that was shown by 1D ^{1}H NMR to change in intensity between the different Ports to be provisionally assigned as a disaccharide.

The aromatic region of the 1D NMR spectra of the Port wines is that with the lowest signal-to-noise ratio, requiring a minimum of 128 transients for reasonable HR-DOSY spectra to be obtained. The low apparent diffusion coefficients seen for Port B and C peaks in the 6.5−7.5 ppm region (around 1×10^{-10} m^2/s) (**Figure 5B,C**) clearly indicate that much of the signal observed originates from slowly diffusing species, most probably corresponding to the anthocyanin-based polymers mentioned above. As expected, most of these slowly diffusing species are absent from Port A, in which the DOSY signals in the same region show apparent diffusion constants at and above 3×10^{-10} m^2/s. This observation, together with the observed increase in concentration in Port A of formic acid (peak 1) and of unassigned rapidly diffusing compounds (signals 3 and 4), indicates that some of the large aromatic species precipitate or break down during aging. For globular molecules of fixed density, diffusion coefficient scales as the cube root of relative molecular mass, M_r. Under these assumptions and using formic acid (peak 1) and ethanal (peak 2) as calibrants, the two singlets at 8.12 and at 9.45 ppm show apparent diffusion coefficients that are consistent with M_r values roughly on the order of 70 and 190 Da, respectively. The latter signal remains unassigned, but the former shows a good match in both chemical shift and diffusion coefficient with ethyl formate (MW 72), for which the concentration is known to increase with age in Port wine (*1*). This illustrates the potential usefulness of DOSY for the interpretation of weak NMR singlets, which can be difficult to assign solely on the basis of chemical shift. The same calculation applied to the apparent diffusion coefficient for the broad aromatic envelope around 7 ppm (0.8×10^{-10} m^2/s) yields a size estimate for these species in the tens of kilodaltons range. Further evidence for the breakdown or other loss of large aromatics is seen in the absence in Port A of the DOSY peaks at just under 6 ppm (**Figure 5B**) and of the slowly diffusing peak at 9.15 ppm, which is clearly visible in both Ports B and C (**Figure 5B,C**). Finally, peak 5 in **Figure 5A** indicates the relative increase in concentration of *p*-hydroxybenzoic acid that was noted earlier by 2D NMR; this assignment is further supported by the observed diffusion coefficient of 4.5×10^{-10} m^2/s, which is consistent with the MW of the acid.

In conclusion, DOSY has provided valuable information about the sizes of the molecules present in the Port wines studied, confirming many of the assignments carried out by high-resolution NMR but also revealing important information about further compounds. In particular, DOSY has enabled (a) the detection of low abundance disaccharides, not currently assignable because of overlap with strong signals arising from the major carbohydrates glucose and fructose (3D DOSY should

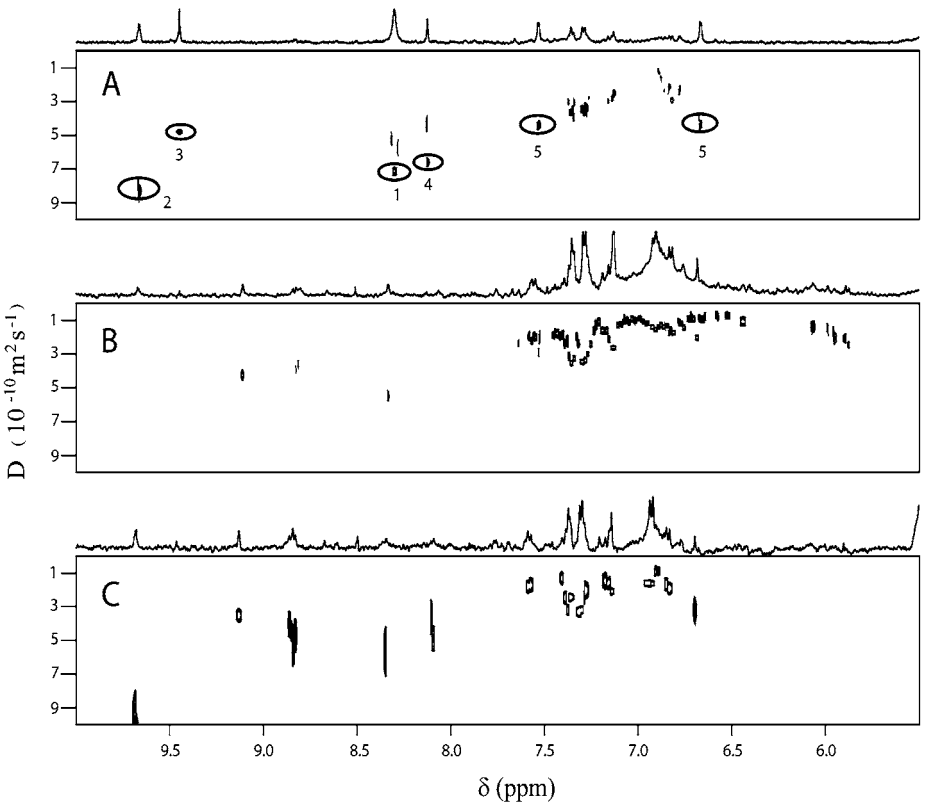

Figure 5. DOSY spectra of the 5.5–10.0 ppm region for (**A**) Port A (20 years old), (**B**) Port B (3 years old), and (**C**) Port C (1 year old). Some signals mentioned in the text are highlighted: (1) formic acid, (2) ethanal, (3) unidentified (M_w ca. 190), (4) unidentified (M_w ca. 70, possibly ethyl formate), and (5) *p*-hydroxy benzoic acid.

be of use here), (b) the detection in the younger Ports of large aromatic species with diffusion coefficients consistent with sizes in the tens of kilodaltons range, and (c) the identification in the oldest Port of small molecules resonating as singlets in the aromatic region, which include ethyl formate and several other unassigned compounds. The most notable difference found among the wines of different ages was the decrease in the concentration of polyphenolic molecules with age with the simultaneous appearance of new small compounds reflecting the expected molecular breakdown occurring with wine aging. Although the contribution of other variables, such as making and storage processes or characteristics of harvest year, toward the composition of the wine must be allowed for, the general agreement between the changes noted and the expected effects of wine aging indicates that most changes are indeed mainly due to the different wine ages. DOSY results enabled an approximate MW estimate to be made for the polyphenolic molecules in the young Ports, suggesting that DOSY may have the potential to characterize the evolution of polyphenol size with aging. In addition, the possible identification of peaks in different spectral regions sharing the same diffusion coefficient may, potentially, provide information on the existence of specific linkages, for example, aromatic−carbohydrate linkages; this is the subject of ongoing work.

The limitations of the DOSY technique become obvious in regions of strong spectral overlap; however, improvements are expected to be achievable with 3D DOSY techniques, which spread resonances over two frequency dimensions, reducing the degree of overlap. Another possibility, which carries the penalty of much poorer resolution in the diffusion dimension, is to attempt to resolve the overlapping exponential decays using various approximations to the inverse Laplace transform (*26*).

ACKNOWLEDGMENT

The authors thank the Port Wine Institute, Portugal, for providing the samples, together with chemical analysis data.

LITERATURE CITED

(1) Silva Ferreira, A. C. Caractérisation du vieillissement du Vin de Porto. Approche chimique et statistique. Role aromatique do Sotolon. Thèse de Doctorat de l'Université de Bordeaux II, 1998.

(2) Gil, A. M.; Le Duarte, I. F.; Godejohann, M.; Braumann, U.; Maraschin, M.; Spraul, M. Characterization of the aromatic composition of some liquid foods by nuclear magnetic resonance spectrometry and liquid chromatography with nuclear magnetic resonance and mass spectrometric detection. *Anal. Chim. Acta* **2003**, *488*, 35−51.

(3) Ramos, A.; Santos, H. NMR studies of wine chemistry and wine bacteria. *Annu. Rep. NMR Spectrosc.* **1999**, *37*, 179−202.

(4) Duarte, I. F.; Godejohann, M.; Braumann, U.; Spraul, M.; Gil, A.M. Application of NMR spectroscopy and LC-NMR/MS to the identification of carbohydrates in beer. *J. Agric. Food Chem.* **2003**, *51*, 4847−4852.

(5) Lu, Y. R.; Foo, L. Y. The polyphenol constituents of grape pomace. *Food Chem.* **1999**, *65*, 1−8.

(6) Gil, A. M.; Duarte, I. F.; Delgadillo, I.; Colquhoun, I. J.; Casuscelli, F.; Humpfer, E.; Spraul, M. Study of the compositional changes of mango during ripening by use of nuclear magnetic resonance spectroscopy. *J. Agric. Food Chem.* **2000**, *48*, 1524−1536.

(7) Kosir, I. J.; Kidric, J. Identification of amino acids in wines by one- and two- dimensional nuclear magnetic resonance spectroscopy. *J. Agric. Food Chem.* **2001**, *49*, 50−56.

(8) Kosir, I. J.; Kidric, J. Use of modern nuclear magnetic resonance spectroscopy in wine analysis: Determination of minor compounds. *Anal. Chim. Acta* **2002**, *458*, 77−84.

(9) Duarte, I.; Barros, A.; Belton, P. S.; Righelato, R.; Spraul, M.; Humpfer, E.; Gil, A. M. High-resolution nuclear magnetic resonance spectroscopy and multivariate analysis for the characterization of beer. *J. Agric. Food Chem.* **2002**, *50*, 2475−2481.
(10) Martin, G. J.; Mazure, M.; Jouitteau, C.; Martin, Y. L.; Aguile, L.; Allain, P. Characterization of the geographic origin of Bordeaux wines by a combined use of isotopic and trace element measurements. *Am. J. Enol. Vitic.* **1999**, *50*, 409−417.
(11) Kosir, I. J.; Kocjancic, M.; Ogrinc, N.; Kidric, J. Use of SNIF-NMR and IRMS in combination with chemometric methods for the determination of chaptalisation and geographical origin of wines (the example of Slovenian wines). *Anal. Chim. Acta* **2001**, *429*, 195−206.
(12) Ogrinc, N.; Kosir, I. J.; Kocjancic, M.; Kidric, J. Determination of authenticy, regional origin, and vintage of Slovenian wines using a combination of IRMS and SNIF-NMR analyses. *J. Agric. Food Chem.* **2001**, *49*, 1432−1440.
(13) Ogrinc, N.; Kosir, I. J.; Spangenberg, J. E.; Kidric, J. The application of NMR and MS methods for detection of adulteration of wine, fruit juices, and olive oil. A review. *Anal. Bioanal. Chem.* **2003**, *376*, 424−430.
(14) Johnson, C. S. Diffusion ordered nuclear magnetic resonance spectroscopy: Principles and applications. *Nucl. Magn. Reson. Spectrosc.* **1999**, *34*, 203−256.
(15) Morris, K. F.; Johnson, C. S. Diffusion-ordered 2-dimensional nuclear-magnetic-resonance spectroscopy. *J. Am. Chem. Soc.* **1992**, *114*, 3139−3141.
(16) Morris, G. A. Diffusion-Ordered Spectroscopy (DOSY). In *Encyclopedia of Nuclear Magnetic Resonance*; Grant, D. M., Harris, R. K., Eds.; John Wiley & Sons Ltd: Chichester, U.K., 2002; pp 35−44.
(17) Barjat, H.; Morris, G. A.; Smart, T. S.; Swanson, A. G.; Williams, S. C. R. High-resolution diffusion-ordered 2D spectroscopy (HR-DOSY) − A new tool for the analysis of complex mixtures. *J. Magn. Reson. B* **1995**, *108*, 170−172.
(18) Sobolev, A. P.; Segre, A.; Lamanna, R. Proton high-field NMR study of tomato juice. *Magn. Reson. Chem.* **2003**, *41*, 237−245.
(19) Gil, A. M.; Duarte, I.; Cabrita, E.; Goodfellow, B. J.; Spraul, M.; Kerssebaum, R. Exploratory applications of Diffusion Ordered Spectroscopy (DOSY) to liquid foods: An aid towards spectral assignment. *Anal. Chim. Acta* **2004**, *506*, 215−223.
(20) Bax, A.; Davis, D. G. MLEV-17-Based Two-Dimensional Homonuclear Magnetization Transfer Spectroscopy. *J. Magn. Reson.* **1985**, *65*, 355−360.
(21) Pelta, M. D.; Morris, G. A.; Stchedroff, M. J.; Hammond, S. J. A one-shot sequence for high-resolution diffusion-ordered spectroscopy. *Magn. Reson. Chem.* **2002**, *40*, S147−S152.
(22) Morris, G. A.; Barjat, H.; Horne, T. J. Reference Deconvolution Methods. *Prog. Nucl. Magn. Reson. Spectrosc.* **1997**, *31*, 197−257.
(23) Morris, G. A. Compensation of instrumental imperfections by deconvolution using an internal reference signal. *J. Magn. Reson.* **1988**, *80*, 547−552.
(24) Bakker, J. The analysis of Port wines by high performance liquid chromatography. *Int. Analyst* **1988**, *2*, 28−33.
(25) Bakker, J.; Picinelli, A.; Bridle, P. Model wine solutions: Colour and composition changes during aging. *Vitis* **1993**, *32*, 111−118.
(26) Antalek, B. Using pulsed gradient spin−echo NMR for chemical mixture analysis: How to obtain optimum results. *Concepts Magn. Reson.* **2002**, *14*, 225−258.

Received for review February 5, 2004. Revised manuscript received April 7, 2004. Accepted April 14, 2004. The authors thank the Royal Society, U.K., for a European Study Visit Grant. M. Nilsson thanks the Foundation for Science and Technology, Portugal, for funding support through the Grant SFRH/B PD/6561/2001 within the III Community framework.

JF049797U